

A subpopulation of nociceptors specifically linked to itch

Liang Han¹, Chao Ma^{2,3}, Qin Liu^{1,4}, Hao-Jui Weng^{1,4}, Yiyuan Cui⁵, Zongxiang Tang^{1,4}, Yushin Kim¹, Hong Nie^{3,6}, Lintao Qu³, Kush N Patel^{1,4}, Zhe Li¹, Benjamin McNeil¹, Shaoqiu He⁷, Yun Guan⁷, Bo Xiao⁵, Robert H LaMotte³ & Xinzhong Dong^{1,4}

Itch-specific neurons have been sought for decades. The existence of such neurons has been doubted recently as a result of the observation that itch-mediating neurons also respond to painful stimuli. We genetically labeled and manipulated *MrgprA3*⁺ neurons in the dorsal root ganglion (DRG) and found that they exclusively innervated the epidermis of the skin and responded to multiple pruritogens. Ablation of *MrgprA3*⁺ neurons led to substantial reductions in scratching evoked by multiple pruritogens and occurring spontaneously under chronic itch conditions, whereas pain sensitivity remained intact. Notably, mice in which TRPV1 was exclusively expressed in *MrgprA3*⁺ neurons exhibited itch, but not pain, behavior in response to capsaicin. Although *MrgprA3*⁺ neurons were sensitive to noxious heat, activation of TRPV1 in these neurons by noxious heat did not alter pain behavior. These data suggest that *MrgprA3* defines a specific subpopulation of DRG neurons mediating itch. Our study opens new avenues for studying itch and developing anti-pruritic therapies.

Pain and itch are two basic modalities that are initiated and mediated by primary sensory neurons with cell bodies in the DRG or trigeminal ganglia. These neurons are highly diverse on the basis of their somal sizes, expression of ion channels and receptors, innervation territories, and electrophysiological properties¹. Small-diameter DRG neurons with unmyelinated axons (C fibers) are major neuronal types for mediating pain and itch^{1,2}. The sensations of pain and itch are distinct, and each can elicit different behavioral responses, such as withdrawal (to avoid tissue injury) and scratching (to remove irritants), respectively. This leads to the fundamental question of whether there are DRG neurons whose primary function is to elicit itch, but not pain. Three important criteria should be met for neurons to be considered itch specific. First, these neurons should respond to itchy stimuli (pruritogens). Second, specific loss of these neurons should lead to a reduction in itch, but not pain. Third, and most importantly, specific activation of these neurons should evoke itch, but not pain.

There is ample evidence for different types of primary cutaneous neurons that respond to stimuli that elicit itch sensations in human and itch-associated behavior in animals. These neurons are subsets of nociceptive neurons that also respond to chemical, mechanical or heat stimuli that elicit pain in humans or pain behavior in animals and not itch or itch behavior. For example, in human nerve, there are mechanically insensitive cutaneous C fibers whose responses to histamine correspond to the itch produced³, but which also respond to noxious heat and/or one or more painful chemicals such as capsaicin⁴.

There are other C fibers in humans, monkeys and mice that respond to heat and mechanical noxious stimuli, but whose responses to cowhage spicules correspond to the histamine-independent itch this stimulus produces^{5–9}. Given that neurons that are responsive to pruritic chemical agents such as histamine are also activated by painful stimuli, there is uncertainty as to whether their function is specific to the mediation of itch. The major hurdle to further investigation is the lack of specific molecular markers for labeling these neurons and molecular methods of manipulating their contribution to itch.

Previously, we found that certain *Mrgpr* genes, encoding a large family of G protein-coupled receptors, specifically expressed in subsets of small-diameter DRG neurons, function as receptors for certain pruritogens and mediate itch-associated behavior (scratching) accordingly. For example, *MrgprA3* is a receptor for the anti-malarial drug chloroquine and mediates its direct activation of DRG neurons and chloroquine-induced site-directed scratching^{10,11}. Bovine adrenal medulla peptide 8–22 (BAM8–22) and SLIGRL-NH₂, each capable of eliciting a histamine-independent itch, act through *MrgprC11* (refs. 11–13). Given that the expression of *MrgprA3* and *MrgprC11* largely overlaps in DRG neurons¹⁴, most chloroquine-sensitive neurons also respond to BAM8–22 and SLIGRL-NH₂^{11,13}. As histamine can activate all chloroquine-sensitive neurons, *MrgprA3*⁺ neurons therefore respond to at least four different pruritogens¹¹. Thus, *MrgprA3*⁺ neurons are good candidates as neurons specifically dedicated to eliciting itch and itch-associated behavior. To test

¹The Solomon H. Snyder Department of Neuroscience, Center for Sensory Biology, Johns Hopkins University School of Medicine, Baltimore, Maryland, USA.

²Department of Anatomy, Histology and Embryology, Institute of Basic Medical Sciences, Chinese Academy of Medical Sciences, School of Basic Medicine, Peking Union Medical College, Beijing, China. ³Department of Anesthesiology, Yale University School of Medicine, New Haven, Connecticut, USA. ⁴Howard Hughes Medical Institute, Johns Hopkins University School of Medicine, Baltimore, Maryland, USA. ⁵The State Key Laboratory of Biotherapy, West China Hospital, Sichuan University, Chengdu, People's Republic of China. ⁶Guangdong Province Key Laboratory of Pharmacodynamic Constituents of TCM and New Drugs Research, College of Pharmacy, Jinan University, Guangzhou, China. ⁷Department of Anesthesiology and Critical Care Medicine, School of Medicine, Johns Hopkins University, Baltimore, Maryland, USA. Correspondence should be addressed to R.H.L. (robert.lamotte@yale.edu) or X.D. (xdong2@jhmi.edu).

Received 10 September; accepted 26 November; published online 23 December 2012; doi:10.1038/nn.3289

this hypothesis, we generated a transgenic mouse line in which Cre recombinase is specifically expressed in MrgprA3⁺ neurons. Using this genetic tool, we found that MrgprA3 expression defines a specific population of itch-mediating neurons and determined the molecular identity and cellular properties of these neurons.

RESULTS

Generation of *Mrgpra3*^{GFP-Cre} transgenic mouse line

To investigate the function of MrgprA3⁺ neurons, we generated a bacterial artificial chromosome (BAC) transgenic mouse line in which the GFP-Cre fusion protein was expressed under the control of the *Mrgpra3* promoter (Fig. 1). The *Mrgpra3*^{GFP-Cre} transgenic line was fertile and showed no obvious phenotypic or behavioral abnormalities. We crossed *Mrgpra3*^{GFP-Cre} mice with Cre-dependent *ROSA26*^{tdTomato} reporter mice¹⁵ in which Cre-active neurons are marked by the expression of tdTomato (Fig. 1a). Because of the strong fluorescence of tdTomato, these neurons can be visualized directly by epifluorescence without immunohistochemical staining (Fig. 1c,e,h). We used antibodies to GFP to stain adult DRG sections from *Mrgpra3*^{GFP-Cre}; *ROSA26*^{tdTomato} mice. All GFP and tdTomato signals were colocalized in a subset of small-diameter sensory neurons (312 double-labeled neurons from 3 mice; Fig. 1b–d). To characterize Cre activity in the MrgprA3⁺ neurons, we performed *Mrgpra3* *in situ* hybridization on DRG sections from *Mrgpra3*^{GFP-Cre}; *ROSA26*^{tdTomato} mice. We collected tdTomato fluorescent images and bright field images of each DRG section before the *in situ* procedure and matched them to the same DRG section afterward (Fig. 1e,f). Of the tdTomato⁺ neurons examined (389 neurons from 3 mice), 97.2 ± 0.6% exhibited the MrgprA3 *in situ* signal and 95.5 ± 0.5% of these MrgprA3⁺ *in situ* neurons (396 MrgprA3⁺ neurons from 3 mice) were also tdTomato⁺, suggesting that the expression of GFP-Cre is tightly controlled by the endogenous *Mrgpra3* promoter.

Previously, we found that chloroquine activates MrgprA3 and induces calcium influx and action potentials in dissociated MrgprA3⁺ neurons¹¹. To further characterize the *Mrgpra3*^{GFP-Cre} transgenic line, we used Ca²⁺ imaging to examine the responses of dissociated GFP-Cre-labeled DRG neurons to chloroquine. Of the 112 tdTomato⁺ neurons obtained from three *Mrgpra3*^{GFP-Cre}; *ROSA26*^{tdTomato} mice, 90.8 ± 4.6% showed robust increases in intracellular Ca²⁺ following chloroquine application (Fig. 1g–j). In whole-cell patch-clamp recording, 10 of 11 GFP-Cre⁺ neurons from *Mrgpra3*^{GFP-Cre} transgenic mice displayed a train of action potentials following chloroquine treatment.

Figure 1 Generation of the *Mrgpra3*^{GFP-Cre} transgenic mouse line. (a) Diagram showing the mating strategy. (b–d) DRG sections from an *Mrgpra3*^{GFP-Cre}; *ROSA26*^{tdTomato} mouse stained with antibody to GFP. tdTomato fluorescence was visualized directly without staining. (e) Merged image of tdTomato fluorescence and bright field view of a DRG section from a *Mrgpra3*^{GFP-Cre}; *ROSA26*^{tdTomato} mouse. (f) *In situ* hybridization with an *Mrgpra3* probe on the section shown in e. (g–j) Representative light view (g), fluorescent view (h) and Fura-2 ratiometric images of tdTomato⁺ DRG neurons labeled as 1, 2 and 3 (i,j). The color of the neurons switching from yellow to green indicates an increase of the intracellular calcium concentration. (k) Representative traces evoked by chloroquine (CQ, 1 mM) in the calcium imaging assay from the three tdTomato⁺ neurons labeled in j. (l) Representative traces of action potentials induced by chloroquine (1 mM) in neurons from *Mrgpra3*^{GFP-Cre} mice. Chloroquine induced action potentials in GFP-Cre⁺ DRG neurons (10 of 11). In contrast, GFP-Cre⁻ DRG neurons (12) did not show any response to chloroquine. (m) RT-PCR analysis of GFP-Cre expression in various tissues from *Mrgpra3*^{GFP-Cre} mice. GFP-Cre was only detected in the DRG and trigeminal ganglia (TG). *Actb*, β-actin; WT, wild type. All scale bars represent 50 μm.

In contrast, GFP-Cre⁻ neurons failed to generate action potentials after a similar treatment (Fig. 1l). To examine the expression pattern of GFP-Cre, we performed reverse transcription PCR (RT-PCR) with intron-spanning primers on various adult mouse tissues. Among the tissues tested, GFP-Cre was found only in the DRG and trigeminal ganglia, which is consistent with the expression pattern of MrgprA3 (ref. 11; Fig. 1m). Taken together, these data indicate that we successfully generated a transgenic line in which GFP-Cre is specifically expressed in MrgprA3⁺ neurons and that acts as a powerful tool to examine the function of MrgprA3⁺ neurons.

MrgprA3⁺ neurons represent a unique IB4⁺ CGRP⁺ population

Previously, we used *in situ* hybridization to examine the coexpression of MrgprA3 with different molecular markers and found that MrgprA3⁺ neurons are a subset of small-diameter neurons with nociceptive characteristics¹⁶. Using the *Mrgpra3*^{GFP-Cre} transgenic line, we examined the cellular features of MrgprA3 neurons with higher sensitivity. We collected lumbar level 4–6 (L4–L6) DRG sections from *Mrgpra3*^{GFP-Cre}; *ROSA26*^{tdTomato} mice and stained them with antibodies to a number of neuronal markers (Fig. 2a–r). Of the 174 tdTomato⁺ neurons that we examined, 79.1% expressed the nonpeptidergic nociceptive marker IB4 (Fig. 2a–c). For another 130 tdTomato⁺ neurons, 84.7% expressed P2X3 and 97.6% expressed c-RET (Fig. 2d–i). None of the MrgprA3⁺ neurons expressed the peptidergic marker substance P (156 tdTomato⁺ neurons; Fig. 2m–o) or the myelinated neuronal marker neurofilament 200 (NF200, 200 tdTomato⁺ neurons; Fig. 2p–r). In addition, of 184 tdTomato⁺ neurons, 84.2% of MrgprA3⁺ neurons coexpressed another peptidergic marker, calcitonin gene-related peptide (CGRP). CGRP expression appeared to be lower in MrgprA3⁺ neurons than in many other neurons that expressed the peptide (Fig. 2j–l). When DRG sections were stained with antibodies

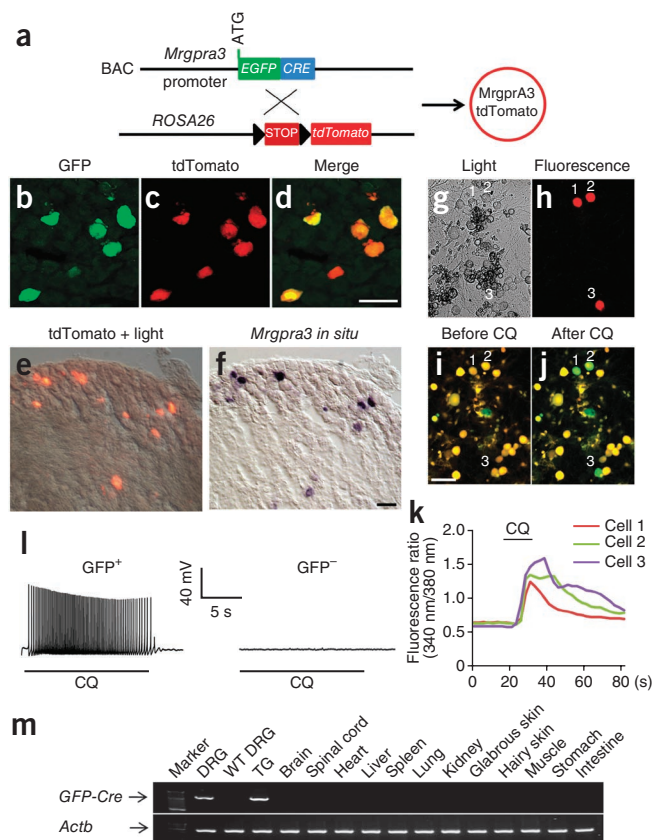
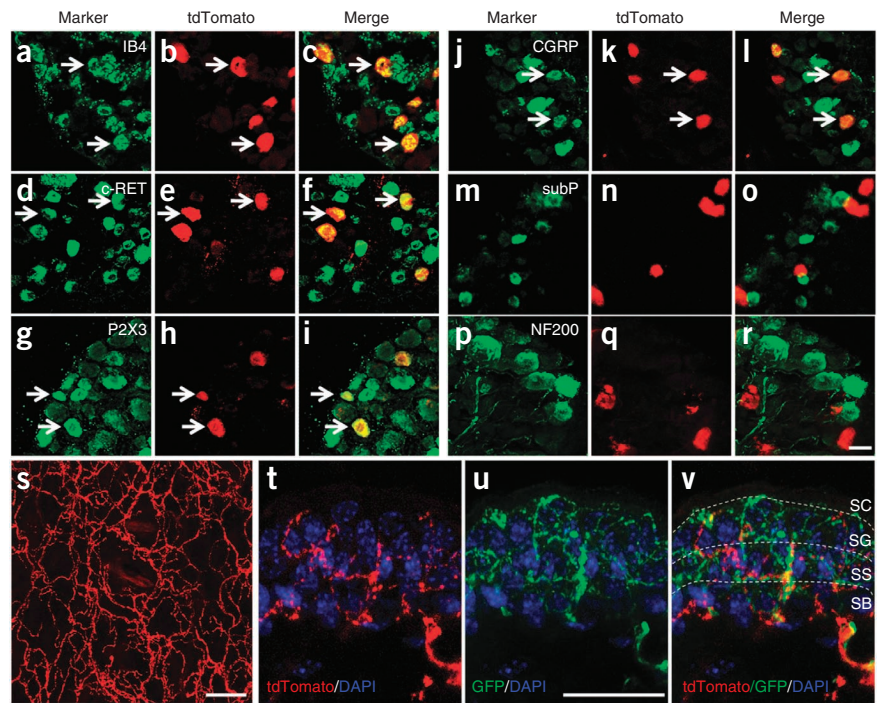


Figure 2 Characterization of MrgprA3⁺ neurons. (a–r) L4–L6 DRG sections from *Mrgpra3^{GFP-Cre}; ROSA26^{tdTomato}* mice stained with the indicated markers. Arrows mark representative double-labeled neurons. (s) Whole-mount imaging of the dorsal thoracic skin from *Mrgpra3^{GFP-Cre}; ROSA26^{tdTomato}* mice showing the distribution of MrgprA3⁺ nerve fibers. (t–v) Section of the dorsal thoracic hairy skin from *Mrgpra3^{GFP-Cre}; ROSA26^{tdTomato}; Mrgprd^{GFP/+}* mice showing MrgprA3⁺ and Mrgprd⁺ free nerve endings in the superficial epidermis. The section was counterstained with DAPI to label nuclei. All scale bars represent 30 μ m. SB, stratum basalis; SC, stratum corneum; SG, stratum granulosum; SS, stratum spinosum. The epidermal subdivisions were identified by keratinocyte nuclear morphology and packing density.



to CGRP and IB4, 63.1% of the MrgprA3⁺ neurons expressed both CGRP and IB4 (106 tdTomato⁺ neurons; **Supplementary Fig. 1a–d**). Thus, MrgprA3⁺ neurons represent a unique population of DRG neurons that are labeled by both the nonpeptidergic marker IB4 and the peptidergic marker CGRP.

In addition, we performed double-labeling experiments using antibodies to TRPV1 and tdTomato in DRG and found that 19% of TRPV1⁺ DRG neurons coexpressed MrgprA3, whereas 88.3% of MrgprA3⁺ neurons coexpressed TRPV1 (**Supplementary Fig. 1e–g**). Furthermore, 93.3% of MrgprA3⁺ neurons expressed MrgprC11 (**Supplementary Fig. 1h–k**).

MrgprA3⁺ neurons exclusively innervate the epidermis

To determine the peripheral targets of MrgprA3⁺ neurons, we examined an extensive array of tissues from *Mrgpra3^{GFP-Cre}; ROSA26^{tdTomato}* mice by visualizing the tdTomato fluorescence of MrgprA3⁺ nerve fiber terminals in the skin and other tissues. We found that MrgprA3⁺ neurons exclusively innervated the epidermis of the skin (**Fig. 2s–v** and **Supplementary Table 1**). MrgprA3⁺ fibers were occasionally seen wrapping around hair follicles. There was also innervation of glabrous skin, although to a lesser extent than in hairy skin. In contrast, MrgprA3⁺ nerve fibers were completely absent from all other tissues examined in the rest of the body, including lung, heart, stomach, muscle and cornea (**Supplementary Table 1**).

A well-known neuronal population that exclusively innervates the epidermis is the Mrgprd-expressing DRG neurons¹⁷. To examine whether Mrgprd⁺ and MrgprA3⁺ fibers innervate distinct regions of the epidermis, we crossed *Mrgpra3^{GFP-Cre}; ROSA26^{tdTomato}* mice with Mrgprd-GFP knock-in mice in which Mrgprd⁺ neurons are labeled with GFP (*Mrgprd^{GFP/+}*)¹⁷. Sections from the hairy skin of *Mrgpra3^{GFP-Cre}; ROSA26^{tdTomato}; Mrgprd^{GFP/+}* mice were collected and stained with antibody to GFP. As Cre is a nuclear protein, the fusion protein of GFP-Cre is present in the nucleus and not in axons. tdTomato is a cytoplasmic protein and therefore fills the entire axon of the neuron. Thus, MrgprA3⁺ fibers in *Mrgpra3^{GFP-Cre}; Rosa26^{tdTomato}* mice were red, rather than yellow (green + red). MrgprA3⁺ fibers (red) could be easily distinguished from Mrgprd⁺ fibers, which were green. We found that MrgprA3⁺ and Mrgprd⁺ fibers represent two distinct nerve fiber populations (**Fig. 2t–v**), which is consistent with previous *in situ* hybridization results showing that *Mrgprd* and *Mrgpra3* are expressed in non-overlapping DRG neurons¹⁸. Both MrgprA3⁺

and Mrgprd⁺ free nerve endings penetrated the epidermis and terminated in the same layer of the superficial skin surface, the stratum granulosum (**Fig. 2t–v**).

The central projections of MrgprA3⁺ fibers co-terminated with IB4⁺ fibers in spinal lamina II_{middle} (**Supplementary Fig. 1l**)¹⁷. This portion of lamina II is ventral to the CGRP⁺ lamina and dorsal to the PKC γ lamina (**Supplementary Fig. 1m–o**). Although we found that MrgprA3⁺ neurons expressed CGRP in cell bodies in the DRG (**Fig. 2j–l**), only minimal overlap between the MrgprA3⁺ central projections and the terminals of other CGRP⁺ neurons was observed (**Supplementary Fig. 1m**). This could be explained by the fact that MrgprA3 expression is restricted to cell bodies with low CGRP expression.

MrgprA3⁺ fibers connect with GRPR⁺ neurons in spinal cord

There is evidence that spinal dorsal horn neurons expressing gastrin-releasing peptide receptor (GRPR) mediate chemically evoked scratching behavior in mice^{19,20}. The ablation of GRPR⁺ neurons abolishes scratching responses to multiple pruritic stimuli without altering behaviors in standard tests of pain behavior, suggesting that GRPR⁺ neurons are dedicated pruriceptive neurons in the CNS²⁰. We asked whether MrgprA3⁺ central fibers form direct connections with GRPR⁺ neurons in the spinal cord (**Fig. 3**). We triple stained spinal cord sections for MrgprA3⁺ fibers (tdTomato), GRPR⁺ neurons and the synaptic contacts between them (via the presynaptic marker synapsin-1). We found that a majority (67%) of GRPR⁺ neurons formed synapses with MrgprA3⁺ primary afferents in dorsal horn (**Fig. 3a–k**).

We then asked whether chloroquine injection could preferentially activate GRPR⁺ neurons. Using c-Fos induction as the marker for chloroquine-responsive neurons in the spinal cord, we examined whether c-Fos colocalized with GRPR. Fos-GFP hemizygous transgenic mice in which the expression of a c-Fos-GFP fusion protein is controlled by the *Fos* promoter²¹ were used for this experiment. We injected 10 μ l of chloroquine into the dorsal calf of the right hindlimb of the Fos-GFP mice and, 90 min after the injection, collected the L3–L5 frozen spinal cord sections and stained them with antibodies to GFP and GRPR. Chloroquine injection induced robust c-Fos expression in the

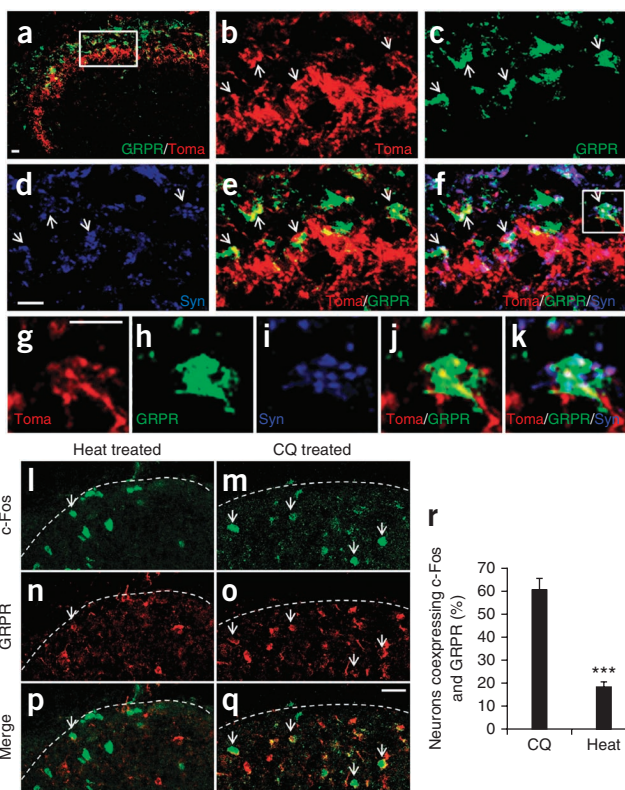


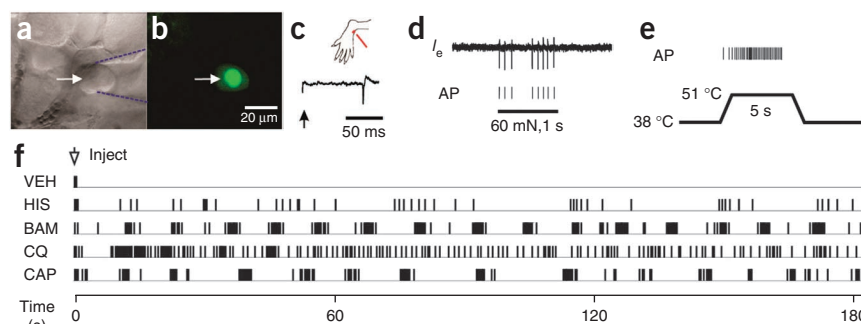
Figure 3 *MrgprA3*⁺ DRG neurons form synaptic connections with GRPR⁺ neurons in the dorsal spinal cord. (**a–k**) Spinal cord cross-sections from the thoracic region of adult *Mrgpra3*^{GFP-Cre}; *ROSA26*^{tdTomato} mice labeled with GRPR (green), tdTomato reporter (Toma; red) and presynaptic marker synapsin 1 (Syn; blue). The boxed area in **a** is shown at greater magnification in **b–f**. The representative neuron in boxed region in **f** is shown at greater magnification in **g–k**. Scale bars represent 10 μ m. Arrows point to representative synaptic connections between tdTomato⁺ nerve fiber and GRPR⁺ neurons. (**l–q**) Double labeling of c-Fos–GFP (green) and GRPR (red) on the L3–L5 spinal cord cross-sections from Fos-GFP mice treated with chloroquine (8 mM) or hot water (50 $^{\circ}$ C). Arrows indicate double-labeled cells. Dashed lines define the boundary of spinal cord sections. (**r**) The percentage of c-Fos⁺ neurons that coexpressed GRPR in the ipsilateral superficial spinal cords. The majority of c-Fos⁺ neurons induced by chloroquine were GRPR⁺ dorsal horn neurons, whereas the majority of heat-induced c-Fos⁺ neurons did not express GRPR ($n = 3$, *** $P = 0.004$). Error bars represent s.e.m. All scale bars represent 10 μ m.

superficial dorsal horn. Notably, $60.9 \pm 4.6\%$ of c-Fos⁺ neurons on the ipsilateral side coexpressed GRPR (three mice, 218 c-Fos⁺ neurons; **Fig. 3m,o,q,r**). In contrast, when we applied hot water (50 $^{\circ}$ C) onto the same region of the skin, only $18.7 \pm 1.7\%$ of the heat-evoked c-Fos⁺ neurons coexpressed GRPR (three mice, 380 c-Fos⁺ neurons; **Fig. 3l,n,p,r**). Taken together, our results indicate that *MrgprA3*⁺ primary afferents form direct synaptic connections with GRPR⁺, specific pruriceptive neurons in the dorsal horn. The different patterns of c-Fos induction by chloroquine (itchy) and noxious heat (painful) provide additional support for our conclusion that *MrgprA3*⁺ neurons in DRG are itch-mediating neurons.

MrgprA3⁺ neurons are cutaneous C-polymodal nociceptors

We then studied *MrgprA3*⁺ neurons in a more physiologically relevant setting with an *in vivo* electrophysiological recording method that we recently developed (**Fig. 4**)²². We first examined *MrgprA3*⁺ neurons

Figure 4 *MrgprA3*⁺ neurons have polymodal nociceptors with C fibers and respond to multiple pruritogens. (**a–f**) *In vivo* electrophysiological recording of *MrgprA3*⁺ neurons. (**a**) Bright-field image of a neuronal recording (arrow) with an extracellular electrode (outlined with dashed blue lines). (**b**) Fluorescent microscopy revealed the expression of GFP (nuclear GFP fluorescence in the *MrgprA3*⁺ neuron). Scale bar in **b** also applies to **a**. (**c**) Location of the cutaneous receptive field (red dot) of this neuron on the hairy skin of the hindpaw and conduction velocity (lower trace, 0.49 m s⁻¹ for the *MrgprA3*⁺ neuron), obtained with electrical stimulation (arrow) of the receptive field, are shown. (**d**) Responses of the neuron to a 60-mN force via a 200- μ m-diameter probe applied to its receptive field (1 s) with original extracellular recording trace (I_e) and each action potential (action potential) indicated by the vertical tick mark below. (**e**) Response to heat stimulation (38–51 $^{\circ}$ C, 5 s) revealed that this was a CMH neuron. (**f**) Responses of the CMH neuron to the intradermal injection for the *MrgprA3* neuron of vehicle (VEH), followed by histamine (HIS, 5.4 mM), BAM8–22 (BAM, 0.2 mM), chloroquine (CQ, 1mM) and capsaicin (CAP, 3.3 mM).



by visualizing GFP-Cre fluorescence in the nuclei and then applying mechanical, heat and chemical stimuli to their cutaneous receptive fields (**Fig. 4a–c,f**). A total of 16 DRG neurons expressing *MrgprA3* were identified. All of these *MrgprA3*⁺ neurons had cutaneous nociceptors with C fibers (conduction velocity range = 0.46–0.81 m s⁻¹; **Fig. 4c**) that responded to both mechanical and heat noxious stimuli (**Fig. 4d,e**; but not to cold, data not shown). They were therefore classified as C-mechanoheat (CMH) polymodal nociceptors.

The following chemicals were injected intradermally into the receptive field in random order: vehicle (saline), histamine, BAM8–22, chloroquine and capsaicin. At least 5 min elapsed between the termination of action potential discharges evoked by one injection and the application of the next. The neurons were silent (that is, not spontaneously active) before each chemical application, and the injection of vehicle ($n = 9$) never evoked any response (that is, no discharges beyond the insertion of the needle). All neurons tested responded to histamine ($n = 9$) and to capsaicin ($n = 9$). Action potentials were evoked by BAM8–22 in eight of ten neurons tested, and by chloroquine in seven of nine neurons (**Fig. 4f**). Cowhage spicules (in groups of 3–5) inserted into the receptive field also evoked responses in all of the neurons that we tested ($n = 4$). In addition, *MrgprA3*⁺ neurons did not respond to β -alanine (50 mM, $n = 9$), an agonist for *MrgprD*, which is expressed in a non-overlapping DRG subpopulation^{16,23}.

Ablation of *MrgprA3*⁺ neurons does not alter pain behavior

One efficient and broadly applicable approach to investigate the function of specific cell populations in the context of the whole organism is to ablate the targeted cell population²⁴. Inducible cell ablation in

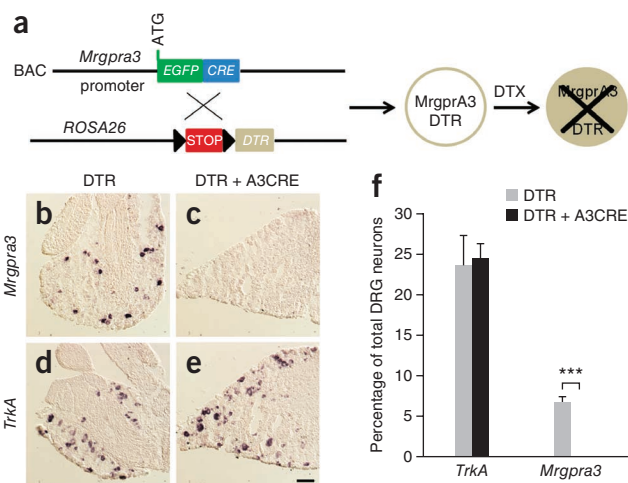


Figure 5 The ablation of MrgprA3⁺ neurons. **(a)** Diagram showing the mating strategy. **(b–e)** *In situ* hybridizations of DRG sections from DTX-treated *Mrgpra3*^{GFP-Cre}; *ROSA26*^{DTR} and *ROSA26*^{DTR} littermates using *Mrgpra3* (**b,c**) and *TrkA* (also known as *Ntrk1*, **d,e**) cDNA probes revealed that MrgprA3⁺ neurons were specifically ablated in *Mrgpra3*^{GFP-Cre}; *ROSA26*^{DTR} mice. Scale bar represents 100 μ m. **(f)** Quantitation of the *in situ* hybridization results ($n = 3$ mice per genotype; *Mrgpra3*, $P = 0.004$; *TrkA*, $P = 0.80$). *** $P < 0.005$, two-tailed unpaired Student's *t* test. Error bars represent s.e.m.

adults is commonly used to avoid compensation during development and can be achieved by expressing human heparin-binding epidermal growth factor-like growth factor precursor (HB-EGF, also referred to as DTR), which is the receptor for the cytotoxic protein diphtheria toxin (DTX)^{25,26}. We selectively ablated MrgprA3⁺ neurons by crossing the *Mrgpra3*^{GFP-Cre} transgenic line with the Cre-dependent *ROSA26*^{DTR} line²⁷, followed by DTX injection (Fig. 5). All of the MrgprA3⁺ neurons were lost 3 weeks after DTX injection (6.8 \pm 0.6% versus 0%; Fig. 5a–c,f). In contrast, the percentage of TrkA⁺ neurons was not changed (23.7 \pm 3.6% versus 24.5 \pm 1.8%; Fig. 5d–f). To confirm the specificity of the ablation, we examined several subpopulations of DRG neurons by staining for various molecular markers. The proportions of CGRP-, IB4-, substance P- and NF200-immunoreactive neurons were similar in DTX-treated *Mrgpra3*^{GFP-Cre}; *ROSA26*^{DTR} mice and *ROSA26*^{DTR} littermates (Supplementary Fig. 2a–o), suggesting that DTX treatment did not produce any general neurotoxic effects.

We tested the responses of *Mrgpra3*^{GFP-Cre}; *ROSA26*^{DTR} mice to acute noxious heat, cold, mechanical and chemical stimulation after DTX administration. DTX-treated *Mrgpra3*^{GFP-Cre}; *ROSA26*^{DTR} mice exhibited equivalent thermal sensitivities as DTX-treated *ROSA26*^{DTR} littermates in the Hargreaves, hot plate, cold plate and tail immersion tests ($n \geq 6$ for each group, $P > 0.5$ for each test; Supplementary Fig. 3a–d). Thus, MrgprA3⁺ neurons are dispensable for normal pain behavior to heat and cold noxious stimuli. Both groups also showed similar mechanical sensitivity as measured by von Frey filament responses (Supplementary Fig. 3e). Injection of capsaicin or formalin into the right hindpaw of the animals evoked comparable licking and flinching behaviors in the DTX-treated *Mrgpra3*^{GFP-Cre}; *ROSA26*^{DTR} mice and

ROSA26^{DTR} littermates (Supplementary Fig. 3f,g). Taken together, these results indicate that MrgprA3⁺ neurons are not required for acute pain sensation. In addition, inflammatory hyperalgesia, induced by complete Freund's adjuvant injected into the paw, was not affected in DTX-treated *Mrgpra3*^{GFP-Cre}; *ROSA26*^{DTR} mice compared with DTX-treated *ROSA26*^{DTR} littermates (Supplementary Fig. 3i,j), suggesting that MrgprA3⁺ neurons are not required for inflammatory pain. Finally, MrgprA3⁺ neuron-ablated mice showed normal motor function as determined by the rotarod test (Supplementary Fig. 2p). Thus, the genetic manipulations leading to the ablation of MrgprA3⁺ neurons had no effects on the neuronal systems mediating pain or motor function.

Ablation of MrgprA3⁺ neurons reduces itch behavior

We next evaluated whether itch-associated behaviors were affected by the ablation of MrgprA3⁺ neurons. Indeed, site-directed scratching in response to the subcutaneous injection of chloroquine into the nape of the neck was significantly reduced in DTX-treated *Mrgpra3*^{GFP-Cre}; *ROSA26*^{DTR} mice compared with DTX-treated *ROSA26*^{DTR} littermates ($P = 0.0005$; Table 1). In addition, the ablation of MrgprA3⁺ neurons also abolished the site-directed scratching induced by BAM8–22 and SLIGRL-NH₂, two pruritogens activating MrgprC11 (Table 1). The total number of scratching bouts exhibited by DTX-treated *Mrgpra3*^{GFP-Cre}; *ROSA26*^{DTR} mice after BAM8–22 or SLIGRL-NH₂ injected into the nape of the neck were comparable to that of the wild-type group injected with saline (SLIGRL, $P = 0.78$; BAM8–22, $P = 0.20$; Table 1). We also tested whether MrgprA3⁺ neurons are required for histamine-induced scratching. Subcutaneous injection of histamine into the nape of the neck induced strong scratching behavior in DTX-treated *ROSA26*^{DTR} mice, whereas DTX-treated *Mrgpra3*^{GFP-Cre}; *ROSA26*^{DTR} mice exhibited a significant decrease in the total number of scratching bouts ($P = 0.005$; Table 1), indicating that MrgprA3⁺ neurons were important for normal histamine-induced scratching behavior. However, these neurons were not the only neurons that were responsive to this chemical, as evidenced by the residual behavior. We tested scratching behaviors evoked by another two pruritogens, alpha-methyl-serotonin (α -Me-5HT) and endothelin-1 (ET-1)²⁸. Both α -Me-5HT- and ET-1-induced scratching behaviors were significantly reduced in the DTX-treated *Mrgpra3*^{GFP-Cre}; *ROSA26*^{DTR} mice ($P = 0.024$) compared with the DTX-treated *ROSA26*^{DTR} littermates ($P = 0.047$; Table 1).

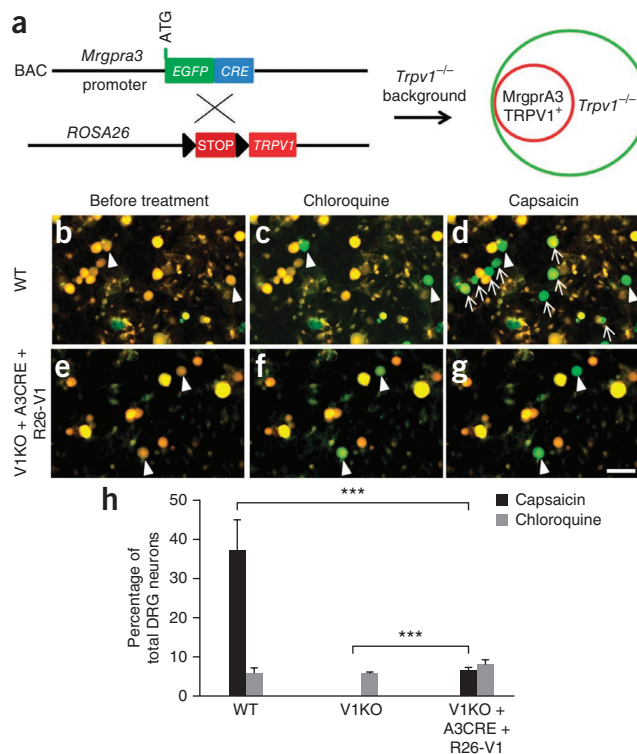
We next examined the role of MrgprA3⁺ neurons in chronic itch conditions by using dry skin and allergic itch mouse models. Dry skin pruritus is a common symptom in patients with xerosis and atopic dermatitis, as well as systemic disorders, including cholestasis and chronic renal failure^{29,30}. Using a murine model for dry skin pruritus³¹,

Table 1 The ablation of MrgprA3⁺ neurons attenuates itch behavior

	Puritogen	DTR (n)	DTR + A3CRE (n)	P value
Neck injection	Saline	12 \pm 5 (7)	11 \pm 3 (7)	0.82
	Chloroquine	236 \pm 25 (5)	65 \pm 25 (6)	0.0005
	SLIGRL	50 \pm 8 (8)	15.6 \pm 7.5 (10)	0.0002
	BAM8–22	90 \pm 12 (7)	5.4 \pm 2.6 (7)	0.0002
	Histamine	60.7 \pm 9.1 (7)	24.2 \pm 6.7 (8)	0.005
	α -Me-5HT	140.5 \pm 18.4 (7)	81.4 \pm 16.7 (7)	0.024
	ET-1	189.8 \pm 52.9 (10)	81.3 \pm 24.5 (8)	0.047
Cheek injection	Chloroquine	66 \pm 20.5 (7)	12.8 \pm 3.6 (6)	0.027
	Histamine	23.6 \pm 4.7 (14)	9.6 \pm 3.3 (11)	0.026
	β -Alanine	29.6 \pm 8.7 (5)	31.5 \pm 3.5 (6)	0.81
Chronic itch condition	Dry skin	138.1 \pm 18.7 (7)	36.6 \pm 11.4 (7)	0.0006
	Allergic itch	147.2 \pm 16.6 (10)	79.3 \pm 19.4 (9)	0.01

Total scratching bouts (mean \pm s.e.m.) in 30 min evoked by injection of different pruritogens or in different chronic itch conditions. n indicates the number of the mice tested. Two-tailed unpaired Student's *t* test was used. The P values refer to the comparison of total scratching bouts evoked by each pruritogen between DTR mice and DTR + A3CRE mice.

Figure 6 Specific activation of *MrgprA3*⁺ neurons. **(a)** Diagram showing the mating strategy. *Mrgpra3*^{GFP-Cre}; *ROSA26*^{Trpv1} mice were generated in a TRPV1 knockout background to exclusively express TRPV1 in *MrgprA3*⁺ neurons. **(b–g)** Fura-2 ratiometric images of cultured DRG neurons from wild-type **(b–d)** and *Trpv1*^{-/-}; *Mrgpra3*^{GFP-Cre}; *ROSA26*^{Trpv1} mice **(e–g)**. The color of the neurons switching from yellow to green indicates the increase of the intracellular calcium concentration **(b–g)**. In wild-type DRG neurons, capsaicin (1 μM) activated a much bigger population than chloroquine (1 mM). However, the percentages of *Trpv1*^{-/-}; *Mrgpra3*^{GFP-Cre}; *ROSA26*^{Trpv1} DRG neurons responding to capsaicin and chloroquine were similar, and every capsaicin-responding neuron responded to chloroquine. Arrowheads point to the neurons responded to both chloroquine and capsaicin. Arrows point to the neurons only responded to capsaicin. Scale bar represents 50 μm. **(h)** The percentage of total DRG neurons from wild-type, *Trpv1*^{-/-} mice, and *Trpv1*^{-/-}; *Mrgpra3*^{GFP-Cre}; *ROSA26*^{Trpv1} mice responded to chloroquine (1 mM) and capsaicin (1 μM). ****P* < 0.005, two-tailed unpaired Student's *t* test. Error bars represent s.e.m.



we found that the spontaneous scratching response decreased significantly after ablation of *MrgprA3*⁺ neurons ($P = 0.0006$; **Table 1**). Itch is always associated with allergic chronic disease, such as allergic conjunctivitis and allergic contact dermatitis^{32–34}. However, little is known of the sensory neurons that mediate allergic itch. In a mouse model of ovalbumin-induced allergic itch³⁰, we found that the ablation of *MrgprA3*⁺ neurons significantly inhibited scratching behaviors ($P = 0.01$; **Table 1**).

Previous reports have shown that mice exhibit distinct behaviors directed to cheek injection of pruritogens versus algogens³⁵. Pruritogens elicit scratching with the hindpaw, whereas algogens evoke facial wiping with the forelimb. This model provides a reliable means of distinguishing pain and itch behaviors. Injection of chloroquine in the cheek evoked robust hindpaw scratching on the cheek in the DTX-treated *ROSA26*^{DTR} mice without any facial wiping. However, the scratching responses were completely abolished in the DTX-treated *Mrgpra3*^{GFP-Cre}; *ROSA26*^{DTR} mice (chloroquine-injected ablated mice, 12.8 ± 3.6 bouts; saline-injected wild-type mice, 6 ± 3.1 bouts; $P = 0.16$; **Table 1**). Hindpaw scratching induced by the administration of histamine in the cheek was also significantly reduced, although not eliminated after the ablation of *MrgprA3*⁺ neurons ($P = 0.026$; **Table 1**). In contrast, facial wiping by the forepaw induced by capsaicin injection was not altered (**Supplementary Fig. 3h**), supporting the conclusion that *MrgprA3*⁺ neurons are specific for mediating itch behavior, but are not required for pain behavior. Recently, we found that intradermal injection of the amino acid β -alanine elicited itch in humans and site-directed scratching in mice³⁶. Consistent with the finding that *MrgprA3* and *MrgprD* define two separate subpopulations of DRG neurons¹⁸, cheek injection of β -alanine also induced a robust scratching response in DTX-treated *Mrgpra3*^{GFP-Cre}; *ROSA26*^{DTR} mice (**Table 1**). The total number of scratching bouts was comparable for the two groups, indicating that *MrgprA3*⁺ neurons are dispensable for β -alanine-induced itch behavior. In summary, the ablation of *MrgprA3*⁺ neurons attenuated itch behaviors not only in acute conditions induced by an array of pruritogens, but also in chronic itch conditions.

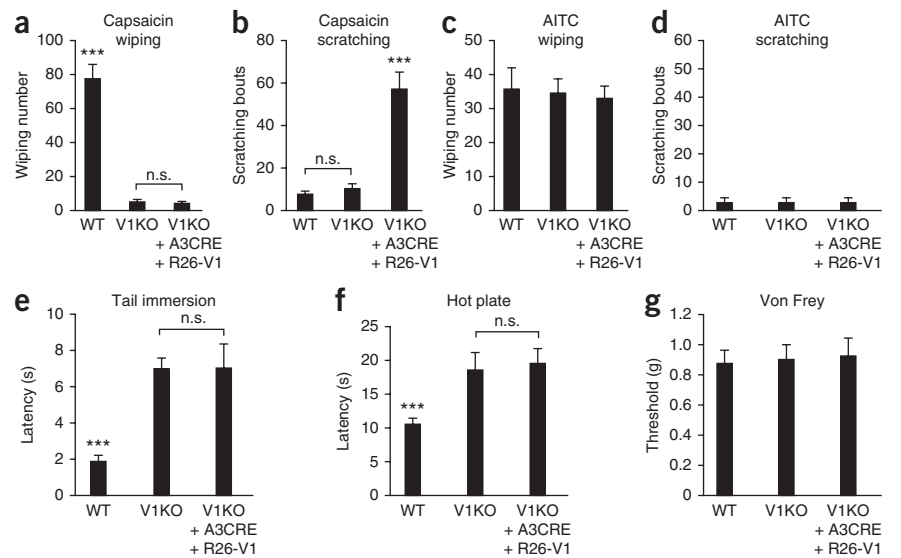
MrgprA3⁺ neurons mediate only itch and not pain behavior

Our findings do not preclude the possibility that *MrgprA3*⁺ neurons may also mediate pain and that their ablation has no substantial effect on pain behavior as a result of compensation from other pain-mediating neurons. One way to rule out this possibility is to selectively activate only *MrgprA3*⁺ neurons with a stimulus that normally elicits pain, but not itch, behavior. If both pain and itch behaviors occur, then the activation of these neurons mediates both types of behavior, whereas if itch behavior alone occurs, then the activation of these

neurons is specifically linked to itch regardless of the type of stimulus that activates the neuron. Our approach was to exclusively express the algogen receptor TRPV1 in *MrgprA3*⁺ neurons. A previous study found that the Cre-dependent *ROSA26*-TRPV1 knock-in mouse line expresses TRPV1 in a specific neuronal population³⁷. In these mice, capsaicin can evoke action potential firing in the targeted neurons and induce behavioral responses^{37,38}. We generated *Trpv1*^{-/-}; *Mrgpra3*^{GFP-Cre}; *ROSA26*^{Trpv1} mice by crossing *Mrgpra3*^{GFP-Cre} mice with *ROSA26*^{Trpv1} mice (to re-express TRPV1 in *MrgprA3*⁺ neurons) in the TRPV1 knockout background (to eliminate TRPV1 from all cells) (**Fig. 6**). We first tested specific functional expression of the *Trpv1* transgene in *MrgprA3*⁺ neurons by calcium imaging using DRG neurons in acute culture. For cultured neurons sampled from wild-type mice ($n = 396$ neurons), *Trpv1*^{-/-} mice ($n = 305$) and *Trpv1*^{-/-}; *Mrgpra3*^{GFP-Cre}; *ROSA26*^{Trpv1} mice ($n = 346$), the incidences of responses to chloroquine were virtually the same (wild type, $5.9 \pm 1.2\%$; *Trpv1*^{-/-}, $5.75 \pm 0.4\%$; *Trpv1*^{-/-}; *Mrgpra3*^{GFP-Cre}; *ROSA26*^{Trpv1}, $8 \pm 1.3\%$; $n = 3$ mice per genotype; **Fig. 6a–c,e,f,h**). We next analyzed the responsiveness of cultured DRG neurons from the three genotypes of mice to capsaicin. Of the DRG neurons from wild-type mice, 37.2% responded to capsaicin. Neurons from *Trpv1*^{-/-} did not respond to capsaicin. However, 6.6% of neurons from *Trpv1*^{-/-}; *Mrgpra3*^{GFP-Cre}; *ROSA26*^{Trpv1} mice responded to capsaicin (**Fig. 6d,g,h**). Notably, every capsaicin-responding neurons from *Trpv1*^{-/-}; *Mrgpra3*^{GFP-Cre}; *ROSA26*^{Trpv1} mice responded to chloroquine (**Fig. 6e–g**), indicating that TRPV1 is exclusively expressed in *MrgprA3*⁺ neurons.

We then used the cheek injection model³⁵ to examine whether pain or itch behaviors or both are triggered by an intradermal injection of capsaicin when TRPV1 is exclusively expressed in *MrgprA3*⁺ neurons (**Fig. 7**). In response to capsaicin injected into the cheek, wild-type mice exhibited robust site-directed wiping (using the forepaw) and little if any scratching (with the hind paw), which is indicative of pain behavior. *Trpv1*^{-/-} mice exhibited neither wiping nor scratching in response to cheek injection of capsaicin. In contrast, *Trpv1*^{-/-}; *Mrgpra3*^{GFP-Cre};

Figure 7 Specific activation of *MrgprA3*⁺ neurons evokes robust scratching and little or no pain response. **(a)** Cheek injection of capsaicin (3.3 mM) induced robust, site-directed wiping with the forepaw in wild-type mice ($n = 13$), but not in *Trpv1*^{-/-} mice (V1KO, $n = 13$) or *Trpv1*^{-/-}; *Mrgpra3*^{GFP-Cre}; *ROSA26*^{Trpv1} mice (V1KO + A3CRE + R26-V1, $n = 10$) (wild type versus V1KO, $P = 1.8 \times 10^{-9}$; V1KO versus V1KO + A3CRE + R26-V1, $P = 0.59$). **(b)** Cheek injection of capsaicin (3.3 mM) induced robust site-directed scratching with the hind paw in *Trpv1*^{-/-}; *Mrgpra3*^{GFP-Cre}; *ROSA26*^{Trpv1} mice ($n = 10$), but not in wild-type ($n = 13$) or *Trpv1*^{-/-} mice ($n = 13$) (wild type versus V1KO, $P = 0.28$; V1KO versus V1KO + A3CRE + R26-V1, $P = 7.2 \times 10^{-7}$). **(c, d)** Cheek injection of allyl isothiocyanate (AITC, 50 mM) induced robust wiping **(c)**, but not scratching **(d)** (wild type, $n = 8$; V1KO, $n = 8$; V1KO + A3CRE + R26-V1, $n = 7$). **(e)** Response latencies of wild-type ($n = 10$), *Trpv1*^{-/-} ($n = 11$) and *Trpv1*^{-/-}; *Mrgpra3*^{GFP-Cre}; *ROSA26*^{Trpv1} mice ($n = 8$) in the tail immersion test (50 °C) (wild type versus V1KO, $P = 2.3 \times 10^{-7}$; V1KO versus V1KO + A3CRE + R26-V1, $P = 0.97$). **(f)** Response latencies in the hot plate tests (55 °C) (wild type, $n = 11$; V1KO, $n = 8$; V1KO + A3CRE + R26-V1, $n = 7$) (wild type versus V1KO, $P = 0.0017$; V1KO versus V1KO + A3CRE + R26-V1, $P = 0.75$). **(g)** Response threshold in the von Frey test (wild type, $n = 10$; V1KO, $n = 10$; V1KO + A3CRE + R26-V1, $n = 8$) (wild type versus V1KO, $P = 0.87$; V1KO versus V1KO + A3CRE + R26-V1, $P = 0.86$). *** $P < 0.005$; two-tailed unpaired Student's *t*-test. n.s., not significant. ($P > 0.05$). Error bars represent s.e.m.



ROSA26^{Trpv1} mice injected with capsaicin exhibited robust site-directed scratching behaviors with little or no wiping (Fig. 7a,b), indicating that the selective activation of *MrgprA3*⁺ neurons by capsaicin elicited itch, but little or no pain. As a control, cheek injection of mustard oil evoked similar numbers of wiping in all three groups of mice with little or no scratching, suggesting that pain sensation mediated by other TRPs (for example, TRPA1) functions normally in *Trpv1*^{-/-}; *Mrgpra3*^{GFP-Cre}; *ROSA26*^{Trpv1} mice (Fig. 7c,d). In addition, these mice showed similar mechanical sensitivity as measured by von Frey filament responses (Fig. 7g).

TRPV1 is essential for detecting noxious heat. As previously shown, *Trpv1*^{-/-} mice exhibited significantly longer tail flick latency in response to 50 °C in the tail immersion test than wild-type mice³⁹ ($P = 2.3 \times 10^{-7}$; Fig. 7e). A similar impaired response was obtained in the hot plate assay³⁹ (Fig. 7f). Notably, *Trpv1*^{-/-}; *Mrgpra3*^{GFP-Cre}; *ROSA26*^{Trpv1} mice have similar latencies in both assays as those in *Trpv1*^{-/-} mice, suggesting that re-introducing TRPV1 in *MrgprA3*⁺ neurons in *Trpv1*^{-/-} mice did not rescue any deficit in sensing noxious heat (Fig. 7e,f).

DISCUSSION

A cellular basis for itch being felt only in the skin

Previously, we found that *MrgprA3* functions as a receptor for the pruritogen chloroquine. Because of its specific expression in DRG, the *Mrgpra3* promoter provides the first means of answering some fundamental questions. Do itch-specific neurons exist? If so, what is the molecular identity of these neurons and what are the cellular and functional properties of these neurons?

One aspect of itch sensation is that itch arises from the skin, but not from deeper tissues, such as muscle, bone and visceral organs, from which pain can be felt. Our results provide a cellular basis of this phenomenon: *MrgprA3*⁺ axons exclusively innervate the skin. It has been suggested that itch-mediating nerve fibers terminate in the superficial skin layer. The traditional algogen, capsaicin, generates pain when delivered intradermally, but can evoke an

initial sensation of itch when applied topically or by means of a cowhage spicule to the skin^{40–42}. One possible explanation is that itch-mediating nerve fibers innervate more superficially and can be chemically activated more selectively by spicule than other fibers that are readily activated by intradermal injection. Indeed, *MrgprA3*⁺ axons penetrate the epidermis and terminate in the stratum granulosum layer.

MrgprA3⁺ neurons mediate multiple types of itch

We found that *MrgprA3*⁺ neurons responded to multiple chemical pruritogens (Fig. 3). The ablation of *MrgprA3*⁺ neurons reduced itch behavior in response to all of the pruritic chemicals that were tested except β -alanine, including those that are known to directly activate *Mrgpr* proteins (chloroquine, BAM 8–22 and SLIGRL)^{11,13} and those that activate other receptors (histamine, ET-1 and α -Me-5HT)^{1,43,44}. In addition, the responsiveness of *MrgprA3*⁺ neurons to algescic stimuli, namely capsaicin, heat and mechanical stimuli, provide a mechanism by which noxious stimuli, such as the punctuate application of such stimuli, might under certain conditions elicit itch. Of clinical relevance is our observation that the spontaneous scratching from dry skin or from allergic responses was substantially attenuated in *MrgprA3*-ablated mice. Together, these data imply that *MrgprA3*⁺ neurons express a broad array of receptors for pruritic stimuli and are involved in mediating both acute and chronic itch.

The insensitivity of *MrgprA3*⁺ neurons to β -alanine and the normal scratching responses to β -alanine in *MrgprA3*-ablated mice also support the existence of multiple types of itch-mediating neurons. In addition, the residual scratching induced by certain pruritogens, especially histamine, ET-1 and α -Me-5HT, in *MrgprA3*-ablated mice indicate that other types of DRG neurons are also involved in mediating itch. For example, at least two types of neurons must mediate histamine-evoked itch behavior, namely *MrgprA3*⁺ neuron and another, as yet unknown type that must contribute to the histamine-evoked scratching in mice that remains after *MrgprA3*⁺ neurons are ablated. Perhaps the latter neurons have properties similar to

the histamine-responsive, mechanically insensitive neurons with C fibers that have been recorded in humans^{3,4}.

TRPV1⁺ neurons belong to parallel pain and itch pathways

Our data indicate that MrgprA3⁺ neurons are also TRPV1⁺ and sensitive to capsaicin and noxious heat. Specific ablation of this subpopulation of TRPV1⁺ neurons did not affect the pain behavior induced by noxious thermal, mechanical and chemical stimuli. Conversely, capsaicin injection in *Trpv1*^{-/-}; *Mrgpra3*^{GFP-Cre}; *ROSA26*^{Trpv1} mice induced scratching, but not wiping, suggesting that the selective activation of the TRPV1⁺ subpopulation expressing MrgprA3 primarily evokes itch, but not pain. In addition, the response latencies to noxious heat of *Trpv1*^{-/-}; *Mrgpra3*^{GFP-Cre}; *ROSA26*^{Trpv1} mice are similar to those of *Trpv1*^{-/-} mice, suggesting that, although MrgprA3⁺ neurons are sensitive to noxious heat, the activation of these neurons by noxious heat did not elicit pain behavior. The specific itch behavior that we obtained by selectively activating only the MrgprA3⁺ neurons provide direct support for the applicability of Muller's 1826 doctrine of specific nerve energies to a submodality of cutaneous sensations, namely the sensation of itch⁴⁵. That is, the quality of sensation evoked by a stimulus depends on the specific neuronal pathway that is activated, regardless of the nature of the stimulus. In this case, if only MrgprA3⁺ neurons are activated by a stimulus, the sensation should be itch even if the stimulus is noxious mechanical, heat or chemical. However, we cannot rule out the possibility that weaker nociceptive sensations that humans typically report as accompanying itch may be present in mice, but of insufficient magnitude to elicit overt pain behavior.

Our findings suggest that nociceptive, capsaicin-sensitive DRG neurons (that express TRPV1) consist of two types: one mediating itch and the other mediating pain. But if this is so, why does the activation of the entire population of TRPV1⁺ neurons by capsaicin (that is, in wild-type mice) only evoke pain and not itch behavior, even though MrgprA3⁺ neurons are also activated? One explanation is that the brain decodes activity in the pruriceptive neurons as itch only when there is minimal activity in the nociceptive neurons that do not mediate itch⁴⁶. Another possibility is that there are central inhibitory mechanisms activated by the pain-mediating neurons that act to block transmission in an itch-mediating pathway^{47–50}. Indeed, in the VGLUT2 conditional knockout mice, in which nociceptors are silenced by disrupting glutamatergic transmission, capsaicin evokes itch rather than pain behavior⁴⁹. It would be important to determine which VGLUT is expressed in MrgprA3⁺ neurons and whether glutamate is essential for itch signaling transmission in these neurons. To study neurons mediating pain from capsaicin injection, we need to develop new genetic tools to specifically manipulate TRPV1⁺ in these neurons (versus itch mediating, for example, MrgprA3⁺ neurons). Currently available DRG-specific Cre lines drive gene expression not only in small-diameter neurons with C fibers, but also in most other types of DRG neurons, including those with large-diameter A β fibers, which would make interpretation of behavioral data difficult.

The search for pruriceptive neurons mediating itch began nearly a century ago. Here, we have defined and characterized a specific subpopulation of itch-mediating neurons, which should open new avenues for advancing itch research as well as foster the development of itch therapies that target this population.

METHODS

Methods and any associated references are available in the [online version of the paper](#).

Note: Supplementary information is available in the [online version of the paper](#).

ACKNOWLEDGMENTS

We thank C. Hawkins and the staff of Transgenic Mouse Core at Johns Hopkins University School of Medicine for assistance with BAC transgenic mouse generation. We thank D. Anderson (California Institute of Technology) and M. Zylka (University of North Carolina at Chapel Hill) for providing *Mrgprd*^{GFP/+} mice and A. Guler (University of Washington) for providing *Rosa26*^{Trpv1} mice. The work was supported by grants from the US National Institutes of Health to X.D. (NS054791 and GM087369), R.L. (NS047399 and NS014624) and Y.G. (NS070814). X.D. is an Early Career Scientist of the Howard Hughes Medical Institute.

AUTHOR CONTRIBUTIONS

L.H. generated the *Mrgpra3*^{GFP-Cre} mice, carried out the genetic manipulation and most of the behavioral, immunostaining and Ca²⁺ imaging experiments, and wrote the manuscript. C.M., H.N. and L.Q. conducted *in vivo* DRG recordings. Q.L., H.-J.W. and K.N.P. contributed to behavioral experiments. Y.C. and B.X. made the MrgprA3-Cre BAC construct. Z.T., Y.K. and Z.L. conducted *in vitro* DRG recordings. B.M., S.H. and Y.G. contributed to immunostaining experiments. R.H.L. and X.D. supervised the project and wrote the manuscript.

COMPETING FINANCIAL INTERESTS

The authors declare no competing financial interests.

Published online at <http://www.nature.com/doi/10.1038/nn.3289>.

Reprints and permissions information is available online at <http://www.nature.com/reprints/index.html>.

- Ikoma, A., Steinhoff, M., Stander, S., Yosipovitch, G. & Schmelz, M. The neurobiology of itch. *Nat. Rev. Neurosci.* **7**, 535–547 (2006).
- Basbaum, A.I., Bautista, D.M., Scherrer, G. & Julius, D. Cellular and molecular mechanisms of pain. *Cell* **139**, 267–284 (2009).
- Schmelz, M., Schmidt, R., Bickel, A., Handwerker, H.O. & Torebjork, H.E. Specific C-receptors for itch in human skin. *J. Neurosci.* **17**, 8003–8008 (1997).
- Schmelz, M. *et al.* Chemical response pattern of different classes of C-nociceptors to pruritogens and algogens. *J. Neurophysiol.* **89**, 2441–2448 (2003).
- Johaneck, L.M. *et al.* A role for polymodal C-fiber afferents in nonhistaminergic itch. *J. Neurosci.* **28**, 7659–7669 (2008).
- Namer, B. *et al.* Separate peripheral pathways for pruritus in man. *J. Neurophysiol.* **100**, 2062–2069 (2008).
- Akiyama, T., Carstens, M.I. & Carstens, E. Facial injections of pruritogens and algogens excite partly overlapping populations of primary and second-order trigeminal neurons in mice. *J. Neurophysiol.* **104**, 2442–2450 (2010).
- Ma, C., Nie, H., Gu, Q., Sikand, P. & LaMotte, R.H. *In vivo* responses of cutaneous C-mechanosensitive neurons in mouse to punctate chemical stimuli that elicit itch and nociceptive sensations in humans. *J. Neurophysiol.* **107**, 357–363 (2012).
- LaMotte, R.H., Shimada, S.G., Green, B.G. & Zeltzman, D. Pruritic and nociceptive sensations and dysesthesias from a spicule of cowhage. *J. Neurophysiol.* **101**, 1430–1443 (2009).
- Wilson, S.R. *et al.* TRPA1 is required for histamine-independent, Mas-related G protein-coupled receptor-mediated itch. *Nat. Neurosci.* **14**, 595–602 (2011).
- Liu, Q. *et al.* Sensory neuron-specific GPCR Mrgprs are itch receptors mediating chloroquine-induced pruritus. *Cell* **139**, 1353–1365 (2009).
- Sikand, P., Dong, X. & LaMotte, R.H. BAM8-22 peptide produces itch and nociceptive sensations in humans independent of histamine release. *J. Neurosci.* **31**, 7563–7567 (2011).
- Liu, Q. *et al.* The distinct roles of two GPCRs, MrgprC11 and PAR2, in itch and hyperalgesia. *Sci. Signal.* **4**, ra45 (2011).
- Zylka, M.J., Dong, X., Southwell, A.L. & Anderson, D.J. Atypical expansion in mice of the sensory neuron-specific Mrg G protein-coupled receptor family. *Proc. Natl. Acad. Sci. USA* **100**, 10043–10048 (2003).
- Madisen, L. *et al.* A robust and high-throughput Cre reporting and characterization system for the whole mouse brain. *Nat. Neurosci.* **13**, 133–140 (2010).
- Dong, X., Han, S., Zylka, M.J., Simon, M.I. & Anderson, D.J. A diverse family of GPCRs expressed in specific subsets of nociceptive sensory neurons. *Cell* **106**, 619–632 (2001).
- Zylka, M.J., Rice, F.L. & Anderson, D.J. Topographically distinct epidermal nociceptive circuits revealed by axonal tracers targeted to Mrgprd. *Neuron* **45**, 17–25 (2005).
- Liu, Y. *et al.* Mechanisms of compartmentalized expression of Mrg class G protein-coupled sensory receptors. *J. Neurosci.* **28**, 125–132 (2008).
- Sun, Y.G. & Chen, Z.F. A gastrin-releasing peptide receptor mediates the itch sensation in the spinal cord. *Nature* **448**, 700–703 (2007).
- Sun, Y.G. *et al.* Cellular basis of itch sensation. *Science* **325**, 1531–1534 (2009).
- Barth, A.L., Gerkin, R.C. & Dean, K.L. Alteration of neuronal firing properties after *in vivo* experience in a FosGFP transgenic mouse. *J. Neurosci.* **24**, 6466–6475 (2004).
- Ma, C., Donnelly, D.F. & LaMotte, R.H. *In vivo* visualization and functional characterization of primary somatic neurons. *J. Neurosci. Methods* **191**, 60–65 (2010).

23. Shinohara, T. *et al.* Identification of a G protein-coupled receptor specifically responsive to beta-alanine. *J. Biol. Chem.* **279**, 23559–23564 (2004).
24. Abrahamsen, B. *et al.* The cell and molecular basis of mechanical, cold and inflammatory pain. *Science* **321**, 702–705 (2008).
25. Naglich, J.G., Metherall, J.E., Russell, D.W. & Eidels, L. Expression cloning of a diphtheria toxin receptor: identity with a heparin-binding EGF-like growth factor precursor. *Cell* **69**, 1051–1061 (1992).
26. Saito, M. *et al.* Diphtheria toxin receptor-mediated conditional and targeted cell ablation in transgenic mice. *Nat. Biotechnol.* **19**, 746–750 (2001).
27. Buch, T. *et al.* A Cre-inducible diphtheria toxin receptor mediates cell lineage ablation after toxin administration. *Nat. Methods* **2**, 419–426 (2005).
28. Imamachi, N. *et al.* TRPV1-expressing primary afferents generate behavioral responses to pruritogens via multiple mechanisms. *Proc. Natl. Acad. Sci. USA* **106**, 11330–11335 (2009).
29. Di Nardo, A., Wertz, P., Giannetti, A. & Seidenari, S. Ceramide and cholesterol composition of the skin of patients with atopic dermatitis. *Acta Derm. Venereol.* **78**, 27–30 (1998).
30. Krajcnik, M. & Zyllicz, Z. Understanding pruritus in systemic disease. *J. Pain Symptom Manage.* **21**, 151–168 (2001).
31. Miyamoto, T., Nojima, H., Shinkado, T., Nakahashi, T. & Kuraishi, Y. Itch-associated response induced by experimental dry skin in mice. *Jpn. J. Pharmacol.* **88**, 285–292 (2002).
32. Saint-Mezard, P. *et al.* Allergic contact dermatitis. *Eur. J. Dermatol.* **14**, 284–295 (2004).
33. Skoner, D.P. Allergic rhinitis: definition, epidemiology, pathophysiology, detection and diagnosis. *J. Allergy Clin. Immunol.* **108**, S2–S8 (2001).
34. Ono, S.J. & Abelson, M.B. Allergic conjunctivitis: update on pathophysiology and prospects for future treatment. *J. Allergy Clin. Immunol.* **115**, 118–122 (2005).
35. Shimada, S.G. & LaMotte, R.H. Behavioral differentiation between itch and pain in mouse. *Pain* **139**, 681–687 (2008).
36. Liu, Q. *et al.* Mechanisms of itch evoked by beta-alanine. *J. Neurosci.* **32**, 14532–14537 (2012).
37. Arenkiel, B.R., Klein, M.E., Davison, I.G., Katz, L.C. & Ehlers, M.D. Genetic control of neuronal activity in mice conditionally expressing TRPV1. *Nat. Methods* **5**, 299–302 (2008).
38. Güler, A.D. *et al.* Transient activation of specific neurons in mice by selective expression of the capsaicin receptor. *Nat. Commun.* **3**, 746 (2012).
39. Caterina, M.J. *et al.* Impaired nociception and pain sensation in mice lacking the capsaicin receptor. *Science* **288**, 306–313 (2000).
40. Sikand, P., Shimada, S.G., Green, B.G. & LaMotte, R.H. Sensory responses to injection and punctate application of capsaicin and histamine to the skin. *Pain* **152**, 2485–2494 (2011).
41. Sikand, P., Shimada, S.G., Green, B.G. & LaMotte, R.H. Similar itch and nociceptive sensations evoked by punctate cutaneous application of capsaicin, histamine and cowhage. *Pain* **144**, 66–75 (2009).
42. Green, B.G. Spatial summation of chemical irritation and itch produced by topical application of capsaicin. *Percept. Psychophys.* **48**, 12–18 (1990).
43. McQueen, D.S., Noble, M.A. & Bond, S.M. Endothelin-1 activates ETA receptors to cause reflex scratching in BALB/c mice. *Br. J. Pharmacol.* **151**, 278–284 (2007).
44. Yamaguchi, T., Nagasawa, T., Satoh, M. & Kuraishi, Y. Itch-associated response induced by intradermal serotonin through 5-HT₂ receptors in mice. *Neurosci. Res.* **35**, 77–83 (1999).
45. Finger, S. & Wade, N.J. The neuroscience of Helmholtz and the theories of Johannes Müller. Part 2. Sensation and perception. *J. Hist. Neurosci.* **11**, 234–254 (2002).
46. McMahon, S.B. & Koltzenburg, M. Itching for an explanation. *Trends Neurosci.* **15**, 497–501 (1992).
47. Lagerström, M.C. *et al.* VGLUT2-dependent sensory neurons in the TRPV1 population regulate pain and itch. *Neuron* **68**, 529–542 (2010).
48. Ross, S.E. *et al.* Loss of inhibitory interneurons in the dorsal spinal cord and elevated itch in Bhlhb5 mutant mice. *Neuron* **65**, 886–898 (2010).
49. Liu, Y. *et al.* VGLUT2-dependent glutamate release from nociceptors is required to sense pain and suppress itch. *Neuron* **68**, 543–556 (2010).
50. Davidson, S. & Giesler, G.J. The multiple pathways for itch and their interactions with pain. *Trends Neurosci.* **33**, 550–558 (2010).

ONLINE METHODS

Mouse lines. We purchased a mouse BAC clone (RP23-311C15) containing the entire *Mrgpra3* gene from the Children's Hospital Oakland Research Institute. We modified the BAC clone using the homologous recombination in bacteria to generate the *Mrgpra3*^{GFP-Cre} mouse line. We purchased *ROSA26*^{TdTomato}, *ROSA26*^{DTR}, *ROSA26*^{Trpv1} and *Trpv1*^{-/-} mouse lines from Jackson Laboratory and crossed them with *Mrgpra3*^{GFP-Cre}. We used the *Mrgpra3*^{GFP-Cre} transgenic line and both reporter mice lines as hemizygotes or heterozygotes for all the experiments.

Behavioral studies. All behavioral tests were performed with an experimenter blind to genotype. The mice were 2–3-month-old males (20–30 g) that had been backcrossed to C57Bl/6 mice for at least six generations. All experiments were performed using protocols approved by the Animal Care and Use Committee of Johns Hopkins University School of Medicine. We injected 5-week-old *Mrgpra3*^{GFP-Cre}; *ROSA26*^{DTR} mice and *ROSA26*^{DTR} littermates with diphtheria toxin (intraperitoneal, 40 µg per kg of body weight, EMD Biosciences) twice, separated by 72 h. Behavioral experiments were performed 3 weeks after the first toxin injection. The day before the behavioral tests, all mice were acclimated for at least 30 min to their testing environment. We housed 4–5 mice in each cage in the vivarium with 12-h light/dark cycle and all the behavioral tests were performed in the morning.

Back injections and cheek injections of chemicals were performed as previously described³⁵. Briefly, pruritic compounds were subcutaneously injected into the nape of the neck for back injection and the right cheek of the animal for the cheek injection after acclimatization. Behavioral responses were video recorded for 30 min. The video recording was subsequently played back in slow motion and the number of bouts of scratching with the hindpaw and, for the cheek, wiping with the forepaw, each directed toward the injection site, were counted.

In the dry skin model, the rostral back of the mice were treated twice daily with cutaneous application of acetone/ether (1:1) mixture followed by water. After a 6-d treatment, the mice showed robust spontaneous scratching and the treated skin area exhibited decreased stratum corneum hydration and increased trans-epidermal water loss, which mimic the symptoms of dry skin in patients^{29,31}. In an allergy model of itch, 50 µg of ovalbumin dissolved in phosphate-buffered saline (PBS) was administered intraperitoneally together with 2 mg of Inject Alum twice, separated by 10 d. We administered 50 µg of ovalbumin dissolved in saline 1 week after the second sensitization in the same manner as other pruritogens, and quantified scratching behavior.

For the hot plate test, a clear glass cylinder was placed on the plate and the mice were placed inside the cylinder. The onset of brisk hindpaw lifts and/or flicking/licking of the hindpaw was assessed at different temperatures.

For the cold plate test, a ceramic plate on a bed of ice was cooled in a –20 °C freezer. During the test, the plate was allowed to warm to 0 °C as measured by two independent temperature probes. The onset of brisk hindpaw lifts and/or flicking/licking of the hindpaw was assessed.

For the tail immersion test, mice were gently restrained in a 50-ml conical tube into which the mice voluntarily entered. The protruding one-third of the tail was then dipped into a water bath of varying temperatures. The latency to respond to the heat stimulus with vigorous flexion of the tail was measured.

For the Hargreaves test, mice were placed under a transparent plastic box (4.5 × 5 × 10 cm) on a glass floor. The infrared source was placed under the glass floor and the infrared light was delivered to the hindpaw. The latency for the animal to withdraw its hindpaw was measured.

For the Von Frey filament test, mice were placed under a transparent plastic box (4.5 × 5 × 10 cm) on a metal mesh. Von Frey filaments, each delivering a different bending force, were applied to the hind paw using the up-down method and the threshold force corresponding to 50% withdrawal was determined.

For the chemically induced pain test, an intraplantar injection was used to administer a total volume of 6 µl of capsaicin (1 mg in 10 ml saline, 7% Tween-80), or formalin (2% formalin in saline, vol/vol). The time mice spent licking and flinching was measured for 15 min after capsaicin injection and for 1 h after formalin injection.

For the rotarod test, each mouse was trained for 5 min at a constant speed of 4 rpm on the rotarod (Rotamex, Columbus Instruments). The first trial started at least 1 h after training. Every day, each mouse received three trials, separated by 30 min, at speeds accelerating from 4 to 40 rpm (with a 4 rpm increase every 30 s). Each mouse was tested for three consecutive days. The trial was finished when the mouse fell off the rotarod. The latency to falling off the rotarod was recorded and used in subsequent analyses.

Cultures of dissociated DRG neurons. DRG from all spinal levels of 3–4-week-old mice were collected in cold DH10 medium and treated with enzyme solution at 37 °C. After trituration and centrifugation, cells were re-suspended in DH10, plated on glass coverslips coated with poly-D-lysine and laminin, cultured in an incubator at 37 °C, and used within 24 h.

Calcium imaging. Calcium imaging was performed as previously described. Briefly, neurons were loaded with Fura 2-acetomethoxy ester (Molecular Probes) for 30 min in the dark at 22 °C. After washing, cells were imaged at 340- and 380-nm excitation to detect intracellular free calcium. Calcium imaging assays were performed with an experimenter blind to genotype.

Whole-cell current-clamp recordings of cultured DRG neurons. Neurons plated on coverslips were transferred into a chamber with the extracellular solution. Patch pipettes had resistances of 2–4 MΩ. In current-clamp recordings, action potential measurements were performed with an Axon 700B amplifier and the pCLAMP 9.2 software package (Axon Instruments). Neurons were perfused with chemicals for 20 s. All experiments were performed at 22 °C.

Immunofluorescence. Adult mice (8–12 weeks old) were anesthetized with pentobarbital and perfused with 20 ml 0.1 M PBS (pH 7.4, 4 °C) followed with 25 ml of fixative (4% formaldehyde (vol/vol) and 14% sat. picric acid (vol/vol) in PBS, 4 °C). Spinal cord and DRG were dissected from the perfused mice. DRG was post-fixed in fixative at 4 °C for 30 min, and spinal cord was fixed for 2 h. Skin was dissected from nonperfused mice and fixed in 2% paraformaldehyde (wt/vol) at 4 °C for 16–18 h. Tissues were cryoprotected in 20% sucrose (wt/vol) for more than 24 h and were sectioned with a cryostat. The sections on slides were dried at 37 °C for 30 min, and fixed with 4% paraformaldehyde at 21–23 °C for 10 min. The slides were pre-incubated in blocking solution (10% normal goat serum (vol/vol), 0.2% Triton X-100 (vol/vol) in PBS, pH 7.4) for 1 or 2 h at 21–23 °C, then incubated overnight at 4 °C with primary antibodies. Secondary antibody incubation was performed at 21–23 °C for 2 h. For primary antibodies, we used rabbit antibody to CGRP (T-4239, Peninsula, 1:1,000), rabbit antibody to NF200 (AB1982, Chemicon, 1:1,000), rabbit antibody to P2X3 (AB5895, Chemicon, 1:1,000), Armenian hamster antibody to c-RET¹⁷ (1:4), rabbit antibody to PKCγ (sc-211, Santa Cruz Biotechnology, 1:1,000), rabbit antibody to GFP (A-11122, Molecular Probes, 1:1,000), chicken antibody to GFP (1:1,000, GFP-1020, Aves Labs) and mouse antibody to Neuronal nuclei (MAB377, Chemicon, 1:300). For secondary antibodies, we used goat antibody to rabbit (A11011, Alexa 568 conjugated; A11008, Alexa 488 conjugated; Molecular Probes), goat antibody to chicken (A11039, Alexa 488 conjugated, Molecular Probes), goat antibody to Armenian hamster (127-165-160, Cy3 conjugated, Jackson Laboratory) and goat antibody to mouse IgG1 (A21124, Alexa 568 conjugated, Molecular Probes). All secondary antibodies were diluted 1:500 in blocking solution. To detect IB4 binding, sections were incubated with *Griffonia simplicifolia* isolectin GS-IB4-Alexa 488 (1:200, A11001, Molecular Probes).

c-Fos induction in the spinal cord. The dorsal calf of the right hindlimb of Fos-GFP mice were shaved 1 d before the experiment. The mice were anesthetized with phenobarbital (200 mg per kg) before treatment. Chloroquine (10 µl of 8 mM) was injected into the dorsal calf. For heat stimulation, one drop of 50 °C water was applied to the shaved dorsal calf ten times, once per minute. The mice were perfused transcardially with 4% paraformaldehyde 90 min after treatment. Frozen spinal cord sections (20 µm) were obtained from the lumbar level (L3–L5) and immunostained for GFP and GRPR (1:100, LS-A831, MBL).

In situ hybridization. Non-isotopic *in situ* hybridization on frozen sections from adult *Mrgpra3*^{GFP-Cre}; *ROSA26*^{TdTomato} mice was performed as previously described using cRNA probes¹⁶. Briefly, *Mrgpra3* cRNA probes were labeled with digoxigenin-UTP. The probes were detected with an alkaline-phosphatase conjugated antibody to digoxigenin (Roche, 1:2,000) and the fluorescent signals were developed using NBT/BCIP substrate.

RT-PCR. Total RNA was extracted from various tissues using Trizol reagent (Invitrogen) according to the manufacturer's instructions. Reverse transcription was carried out using Superscript first strand (Invitrogen). PCR conditions: 95 °C for 3 min, 40 cycles of 30 s at 95 °C, 30 s at 52 °C and 60 s at 72 °C. Intron-spanning

primers were used to avoid genomic contamination. The forward primer is located in the first exon of *Mrgpra3*. The reverse primer is located in the Cre sequence, which is in the second exon of the *GFP-Cre* mRNA in transgenic mice. The sequences of the primers were 5'-TTCTGTAGTGACTGTATCCTTCC TTC-3' (forward) and 5'-CCGTTATTCAACTTGCACCAT-3' (reverse).

***In vivo* electrophysiological recording from cutaneous sensory neurons.**

Adult male mice were used for the *in vivo* electrophysiological recording. The use and handling of animals were approved by the Institutional Animal Care and Use Committee of the Yale University School of Medicine and were in accordance with guidelines provided by the US National Institutes of Health and the International Association for the Study of Pain. Primary sensory neurons innervating the skin on the hindlimb were extracellularly, electrophysiologically recorded using an *in vivo* physiological preparation as described^{8,22}. A peripheral receptive field was identified by exploration of the hindlimb and application of various handheld stimuli. These included the use of a cotton tip (for innocuous

mechanical stimuli), gentle pinching or indentations with a glass probe or von Frey filaments with fixed tip diameters (100 or 200 μm), but delivering different bending forces (for noxious mechanical stimuli), a temperature-controlled chip-resister heating probe, or ice (for noxious temperature stimuli). A series of chemicals were injected into the receptive field, in sequence, each in a volume of 5 μl , and consisting, in random order, of vehicle (0.9% NaCl, wt/vol), histamine (5.4 mM in vehicle), BAM8-22 (0.2 mM), chloroquine (1 mM), and capsaicin (3.3 mM) using a microsyringe with a 31 G needle⁸.

Statistical analysis. Data are presented as mean \pm s.e.m. *n* represents the number of mice analyzed. The distribution of the variables in each experimental group was approximately normal. Statistical comparisons were conducted by two-tailed, unpaired Student's *t* test. Power analysis was used to justify the sample size. Differences were considered to be statistically significant for $P < 0.05$. Representative data are from experiments that were replicated biologically at least three times with similar results.